

Article

Effect of Chicken Egg White-Derived Peptide and Hydrolysates on Abnormal Skin Pigmentation during Wound Recovery

Pei-Gee Yap ¹, Chee-Yuen Gan ^{1,*}, Idanawati Naharudin ^{2,3} and Tin-Wui Wong ^{2,3}

¹ Analytical Biochemistry Research Centre (ABrC), Universiti Sains Malaysia, University Innovation Incubator Building, SAINS@USM Campus, Lebuh Bukit Jambul, Bayan Lepas 11900, Penang, Malaysia

² Non-Destructive Biomedical and Pharmaceutical Research Centre, Smart Manufacturing Research Institute, Universiti Teknologi MARA Selangor, Puncak Alam 42300, Selangor, Malaysia

³ Particle Design Research Group, Faculty of Pharmacy, Universiti Teknologi MARA Selangor, Puncak Alam 42300, Selangor, Malaysia

* Correspondence: cygan@usm.my; Tel.: +604-653-4206

Abstract: Abnormal skin pigmentation commonly occurs during the wound healing process due to the overproduction of melanin. Chicken egg white (CEW) has long been used to improve skin health. Previous published works had found CEW proteins house bioactive peptides that inhibit tyrosinase, the key enzyme of melanogenesis. The current study aimed to evaluate the anti-pigmentation potential and mechanism of the CEW-derived peptide (GYSLGNWVCAAK) and hydrolysates (CEWH_{mono} and CEWH_{di}), using a cell-based model. All of these peptide and hydrolysates inhibited intracellular tyrosinase activity and melanin level up to 45.39 ± 1.31 and $70.01 \pm 1.00\%$, respectively. GYSLGNWVCAAK and CEWH_{di} reduced intracellular cAMP levels by 13.38 ± 3.65 and $14.55 \pm 2.82\%$, respectively; however, CEWH_{mono} did not affect cAMP level. Moreover, the hydrolysates downregulated the mRNA expression of melanogenesis-related genes, such as *Mitf*, *Tyr*, *Trp-1* and *Trp-2*, but GYSLGNWVCAAK only suppressed *Tyr* gene expression. Downregulation of the genes may lower the catalytic activities and/or affect the structural stability of TYR, TRP-1 and TRP-2; thus, impeding melanogenesis to cause an anti-pigmentation effect in the cell. Outcomes from the current study could serve as the starting point to understand the underlying complex, multifaceted melanogenesis regulatory mechanism at the cellular level.

Keywords: bioactive peptide; egg white protein; melanogenesis; skin lightening agent; skin hyperpigmentation



Citation: Yap, P.-G.; Gan, C.-Y.; Naharudin, I.; Wong, T.-W. Effect of Chicken Egg White-Derived Peptide and Hydrolysates on Abnormal Skin Pigmentation during Wound Recovery. *Molecules* **2023**, *28*, 92. <https://doi.org/10.3390/molecules28010092>

Academic Editors: Mansour Sobeh, Mona F. Mahmoud and Daria Maria Monti

Received: 22 November 2022

Revised: 19 December 2022

Accepted: 19 December 2022

Published: 22 December 2022



Copyright: © 2022 by the authors. Licensee MDPI, Basel, Switzerland. This article is an open access article distributed under the terms and conditions of the Creative Commons Attribution (CC BY) license (<https://creativecommons.org/licenses/by/4.0/>).

1. Introduction

Post-inflammatory hyperpigmentation (PIH) is a common acquired hyperpigmentation disorder during the wound healing process as a sequela of cutaneous injury, infection or inflammatory reactions. The hallmark of PIH includes the appearance of flat, dark brown and sometimes blue-grey patches or spots on the wound after its recovery. It can happen to all skin types but tends to affect dark skinned individuals (Fitzpatrick type IV, V and VI, where the skin colour corresponds to olive, brown and black/dark brown, respectively) with greater frequency and severity [1]. Although the exact aetiology of PIH is unclear, hyperpigmentation is associated with the overproduction or deposition of melanin [2,3]. Tyrosinase is the major enzyme in melanogenesis that catalyses the hydroxylation of tyrosine and the oxidation of L-DOPA to *o*-dopaquinone [4]. The *o*-dopaquinone undergoes a series of redox reactions to form dopachrome, where it is then decarboxylated to 5,6-dihydroxyindole (DHI) or enzymatically rearranged into 5,6-dihydroxyindole-2-carboxylic acid (DHICA) by tyrosinase-related protein 2 (TRP-2). DHI and DHICA are polymerised into eumelanin in the presence of tyrosinase-related protein 1 (TRP-1). Both TRP-1 and TRP-2 also function as structural proteins to stabilize tyrosinase and melanosome structures during melanogenesis [5].

Since the overactivity of tyrosinase can induce the overproduction of melanin, inhibition of this enzyme has become the major target to treat or prevent abnormal skin hyperpigmentation [6]. In fact, the global skin lightening product market is expected to reach approximately USD 16 billion by 2030 with a consumer preference shift towards natural, organic-based products [7]. This is because long-term usage of chemical-based products may pose health and safety concerns to consumers, such as cytotoxicity, erythema or dermatitis [8,9], especially when the regulation of skincare products is not as strict compared to prescribed drugs. Therefore, a compound capable of inhibiting tyrosinase activity sourced from natural, organic materials with minimum side effects may favour consumer demand and could be explored for its potential in skin lightening formulations.

Chicken egg white (CEW), apart from being a food source, is a popular ingredient in home skincare remedies. Egg white proteins are rich in bioactive components known as bioactive peptides. Peptides are small, inactive protein fragments encrypted within a parent protein molecule [10]. Peptide-based tyrosinase inhibitors have been reported from various food sources [11,12]. According to the previous studies by our research group, CEW hydrolysates, i.e., 10 mg/mL of CEWH_{mono} and CEWH_{di} inhibited 45.3 ± 0.66 monophenolase and $48.1 \pm 0.23\%$ diphenolase activities of mushroom tyrosinase, respectively [13]. To compare with other reports, the collagen hydrolysate showed 15.44–30.20% tyrosinase inhibition at 5 mg/mL [14]. The jellyfish hydrolysates showed 50% inhibition of tyrosinase activity at 14.1–24.5 mg/mL [15]. The CEWH_{di}-derived peptide, GYSLGNWVCAAK, also gave an IC₅₀ value of 3.04 ± 0.39 mM for tyrosinase diphenolase activity [16], which is more potent than that of FPY [17] and IQSPHFF [18], with IC₅₀ values of 3.22 ± 0.9 and 4.0 mM, respectively. It is of particular interest to further investigate the intracellular anti-pigmentation effect and mechanism of the CEW-derived hydrolysates and peptide in order to evaluate their potential as a skin lightening agent against PIH. Therefore, this work is a follow-up study aimed at determining the effects of GYSLGNWVCAAK, CEWH_{mono} and CEWH_{di} on intracellular tyrosinase activity, melanin level, and cAMP level, and their regulatory role in the melanogenesis signaling pathway using the B16F10 melanoma cell line.

2. Results and Discussion

2.1. Culturing of B16F10 Melanoma Cells

The B16F10 melanoma cell line is commonly used for pigmentation-related studies. This is because human and mouse tyrosinases are highly homologous with 86 and 84% identity at the protein and cDNA levels, respectively [19]. The cell line also shares a similar regulatory mechanism of melanin synthesis with human melanocytes. In addition, the cells can firmly attach to the culture flask and establish a homogenous cell population; thus, allowing microscopic view of cellular differentiation in terms of morphology and melanogenesis [20,21]. The growth morphology of B16F10 melanoma cells is shown in Figure 1a. Upon thawing (Day 0), viable cells with intact cell membranes appeared round and shiny with a hollow ring under a microscope. The cells attached to the culture flask and gradually established their characteristic epithelial-like and spindle shape (Day 1–5). The cells were sub-cultured on Day 6 as the cells had reached >90% confluency. Intracellular melanin production was observed after the third sub-culture (Figure 1b).

2.2. Cell Cytotoxicity Assay

To investigate the cytotoxicity effect of peptide and CEW hydrolysates, B16F10 melanoma cells were administered with various concentrations of GYSLGNWVCAAK, CEWH_{mono} and CEWH_{di} and then subjected to MTT colorimetric assay. According to the ISO 10993-5:2009 guideline, a cellular treatment was considered toxic should it induce a >30% reduction of cell viability [22]. Based on Figure 2, the viability of the cells treated with GYSLGNWVCAAK, CEWH_{mono} and CEWH_{di} were maintained above 75% at 5–100 µg/mL, suggesting an unlikely cytotoxic effect of the samples. In other reports, the milk and rice bran protein-derived peptides even promoted the growth of B16F10 cells at 100–500 µM [23,24]. On the other hand, cell viability decreased significantly ($p < 0.05$) for cells treated with 1000 µg/mL CEWH_{mono}

(20%) and CEWH_{di} (30%) compared to the untreated control. For treatment using the positive control, cell viability dropped beyond 75% at concentrations >10 µg/mL. This cytotoxicity effect could be due to the auto-oxidation of EGCG into hydrogen peroxide and superoxide anion in culture media, which induces oxidative stress to the cells [25]. In short, 100 µg/mL was used as the maximum treatment concentration for GYSLGNWVCAAK, CEWH_{mono} and CEWH_{di} and the results were compared with EGCG at lower levels of 5 and 10 µg/mL in the subsequent analyses.



Figure 1. The (a) growth morphology of B16F10 melanoma cells viewed under 100× magnification and (b) melanin deposition (black arrows) viewed under 200× magnification.

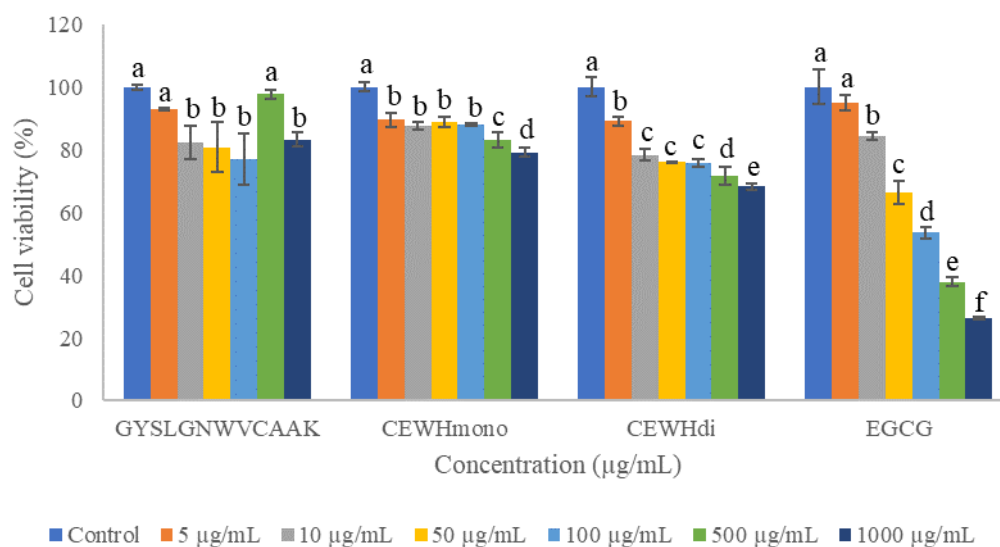


Figure 2. Effects of various concentrations of GYSLGNWVCAAK, CEWH_{mono}, CEWH_{di} and EGCG on the cell viability of B16F10 melanoma cells. Note: Results were reported as the mean \pm standard deviation ($n = 3$); different lowercase letters above the bars indicate significant difference at $p < 0.05$ according to Duncan's test.

2.3. Intracellular Tyrosinase Activity

The tyrosinase activity in B16F10 melanoma cells treated by GYSLGNWVCAAK and CEWH_{di} is shown in Figure 3. To the best of our knowledge, there were no reports on the determination of monophenolase activity using tyrosinase extracted from cell models. This is because it is necessary to first accumulate L-DOPA through diphenolase activity to allow tyrosinase to reach a steady state for full activation of its catalytic activity. Since tyrosinase exists in three oxidation forms, each showing a different ability to catalyze phenol or catechol substrates [26], the kinetics of the monophenolase activity is complicated and difficult to monitor [27]. Therefore, the monophenolase reaction was not determined in the current study.

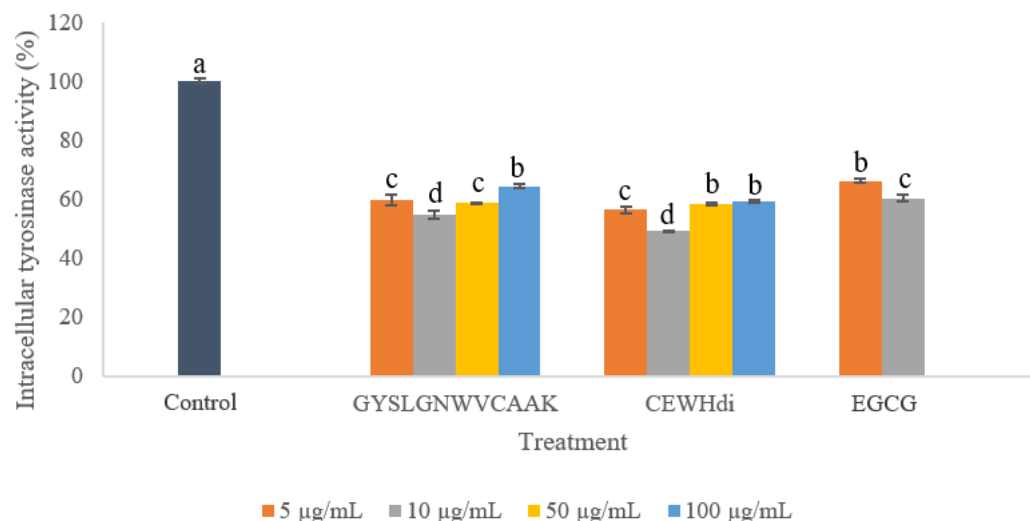


Figure 3. Effects of various concentrations of GYSLGNWVCAAK, CEWH_{di} and EGCG on the intracellular tyrosinase activity of B16F10 melanoma cells. Note: Results were reported as the mean \pm standard deviation ($n = 3$); different lowercase letters above the bars indicate significant difference at $p < 0.05$ according to Duncan's test.

GYSLGNWVCAAK and CEWH_{di} significantly ($p < 0.05$) suppressed the diphenolase activity of B16F10 cells compared to the untreated control in a dose-independent manner.

At 10 $\mu\text{g}/\text{mL}$, GYSLGNWVCAAK and CEWH_{di} gave the highest activity suppression (45.39 ± 1.31 and $50.89 \pm 0.36\%$, respectively), which were higher than the positive control EGCG ($39.65 \pm 1.16\%$) at an equivalent concentration. For 10 $\mu\text{g}/\text{mL}$ of CEWH_{di} treatment, the effect was comparable to 100 $\mu\text{g}/\text{mL}$ of cod skin hydrolysate and 752.4 $\mu\text{g}/\text{mL}$ of milkfish scale hydrolysate, which inhibited 48.93 and 50% of intracellular tyrosinase activities, respectively [28,29]. The effect of 10 $\mu\text{g}/\text{mL}$ (7.88 μM) GYSLGNWVCAAK treatment was higher than that of 350 μM crocodile blood-derived peptides [30]. The inhibitory effect of GYSLGNWVCAAK was ascribed to its direct interactions with tyrosinase and copper-chelating ability, as previously discussed [16]. However, a significant lower inhibition of tyrosinase activity was observed at treatment concentrations >10 $\mu\text{g}/\text{mL}$. The dose-independent inhibition of tyrosinase activity could be due to a different progression between tyrosinase activity and melanin polymerization [31]. To elaborate, the optimal pH of tyrosinase was pH 6.5–7.0 [32], whereas melanin polymerization could be accelerated at alkaline conditions [31]. Since GYSLGNWVCAAK is a basic peptide (isoelectric point, $\text{pI} = \text{pH } 8.77$), increased concentration of the peptide could raise melanosomal microenvironment pH to reduce tyrosinase activity, but at the same time, promote melanin polymerization. The basic side chain of lysine in GYSLGNWVCAAK could act as proton acceptor and centre of clustering for the negatively charged melanin as the polymerization of melanin monomers involves deprotonation [31]. Previous works have shown that basic proteins or peptides can enhance melanin production in vitro [31,33]. Therefore, melanin polymerization may be a more prominent step progressing at a higher rate than tyrosinase catalysis at a higher peptide concentration, triggering higher tyrosinase activity at >10 $\mu\text{g}/\text{mL}$ of peptide.

2.4. Intracellular Melanin Level

The intracellular melanin level of B16F10 melanoma cells treated by various concentrations of GYSLGNWVCAAK, CEWH_{mono}, CEWH_{di} and EGCG is shown in Figure 4. All treatments significantly ($p < 0.05$) lowered the intracellular melanin level compared to the untreated control and the trend of inhibition corresponded to that of intracellular tyrosinase activity (Section 2.3). The intracellular melanin level of B16F10 cells treated with GYSLGNWVCAAK showed a positive correlation, to some extent ($p < 0.10$), with the intracellular tyrosinase activity ($r = 0.845$). The strongest inhibition of intracellular melanin level ($70.01 \pm 1.00\%$) was recorded in B16F10 cells treated with 10 $\mu\text{g}/\text{mL}$ of GYSLGNWVCAAK (Figure 4a). At the same treatment concentration, the inhibition of peptide was more profound than that of EGCG ($40.8 \pm 2.32\%$; Figure 4d). Moreover, this inhibitory effect was >2 -fold stronger than that of crocodile blood-derived peptides [30]. However, at higher treatment concentrations (50 and 100 $\mu\text{g}/\text{mL}$), GYSLGNWVCAAK induced weaker inhibition on melanin synthesis (34.01 ± 1.41 and $23.55 \pm 1.51\%$, respectively). Melanin polymerization may be enhanced by the basic side chain of peptide, as suggested previously (Section 2.3).

For CEWH_{mono} (Figure 4b) and CEWH_{di} (Figure 4c), the intracellular melanin level was the lowest (69.99 ± 1.31 and $47.55 \pm 0.24\%$, respectively) at a treatment concentration of 10 $\mu\text{g}/\text{mL}$. The anti-pigmentation effects of CEWH_{mono} and CEWH_{di} were relatively higher than other reported hydrolysates from cod skin and sea cucumber gelatine [28,34]. A significant ($p < 0.05$) positive correlation was found between the intracellular tyrosinase activity and melanin level of B16F10 cells treated with CEWH_{di} ($r = 0.951$). Since the pH of CEWH_{mono} and CEWH_{di} were 7.95 ± 0.1 and 8.02 ± 0.01 , respectively, the basic property of hydrolysates may favour melanin polymerization, as previously discussed (Section 2.3). In another study, B16F10 cells treated with 0.050, 0.100, 0.210 and 0.638 $\mu\text{g}/\text{mL}$ chicken feather meal hydrolysate resulted in approximately 0, 21, 14 and 5% inhibition of melanin synthesis, respectively [35]. Higher suppression of melanin production (i.e., lower intracellular melanin level) at low treatment concentration, which is similar to the current result, was observed. However, the authors neither determined the pH of hydrolysate nor accounted the effect of pH on intracellular melanin synthesis. Instead, the authors found no correlation

between tyrosinase activity and melanin content as the hydrolysate inhibited the former in a dose-dependent manner but not in the latter. Although this scenario was not observed in the current study, it was noteworthy that melanin inhibition may not always be a direct consequence of tyrosinase inhibition since melanogenesis is a multi-step reaction involving various regulatory players. Based on the results from Sections 2.2–2.4, cellular treatments with 10 $\mu\text{g}/\text{mL}$ of GYSLGNWVCAAK, CEWH_{mono} and CEWH_{di} produced the strongest inhibition of intracellular tyrosinase activity and melanin level without significant cell cytotoxicity. Therefore, 10 $\mu\text{g}/\text{mL}$ of cellular treatment was used in the following analyses.

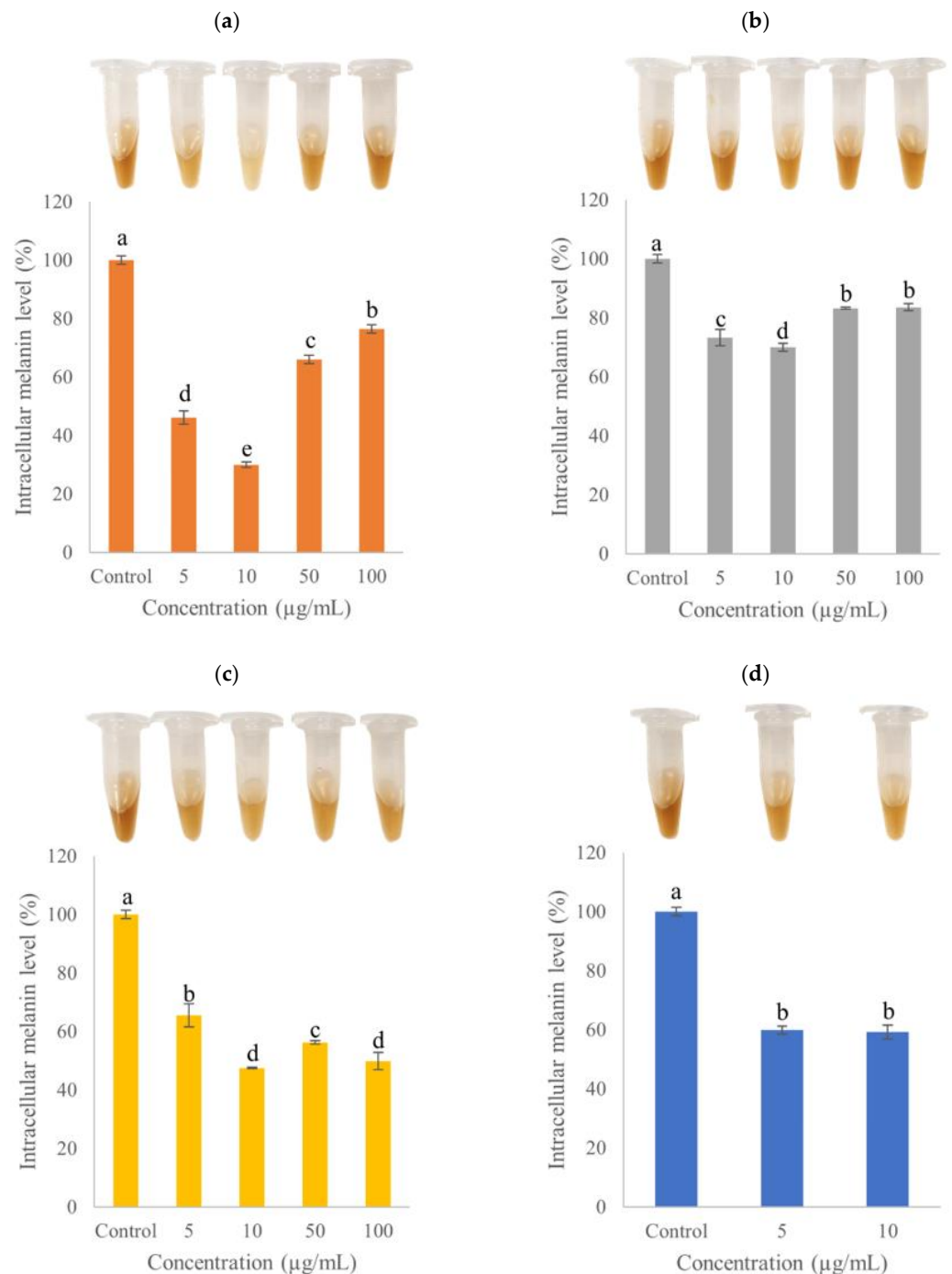


Figure 4. Effects of various concentrations of (a) GYSLGNWVCAAK, (b) CEWH_{mono}, (c) CEWH_{di} and (d) EGCG on the intracellular melanin level of B16F10 melanoma cells. Note: Results were reported as the mean \pm standard deviation ($n = 3$); different lowercase letters above the bars indicate significant difference at $p < 0.05$ according to Duncan's test.

2.5. Intracellular cAMP Level

The intracellular cAMP level of B16F10 melanoma cells treated with 10 µg/mL of GYSLGNWVCAAK, CEWH_{mono}, CEWH_{di} and EGCG is shown in Figure 5. Compared to the untreated control group, GYSLGNWVCAAK, CEWH_{di} and EGCG significantly reduced the cAMP level by 13.38 ± 3.65 ($p < 0.05$), 14.55 ± 2.82 ($p < 0.05$) and $16.04 \pm 5.46\%$ ($p < 0.01$), respectively. The inhibition caused by GYSLGNWVCAAK was slightly lower than that of zebrafish phosvitin-derived peptide Pt5, which reduced 19.0% of cAMP level at 10 µg/mL [36]. In another report, a 48.77% decrement of cAMP level was recorded in B16F10 cells treated with 1.6 mg/mL (2.8 mM) of grass carp scale collagen peptide FTGML [37]. Oyster hydrolysate was also found to reduce cAMP level by approximately 30% at a treatment concentration of 100 µg/mL [38]. An elevated level of intracellular cAMP was associated with upregulation of melanogenesis through the cAMP and/or phosphatidylinositol 3-kinase (PI3K) pathways. Therefore, the current results suggest that GYSLGNWVCAAK, CEWH_{di} and EGCG treatments may impair melanogenesis by lowering the intracellular cAMP level. The cAMP level of B16F10 cells treated with 10 µg/mL of CEWH_{mono}, on the contrary, did not show significant difference ($p > 0.05$) with that of the control group. This indicated that the inhibitory effect of CEWH_{mono} on the intracellular melanin level (Section 2.4) was independent of cAMP.

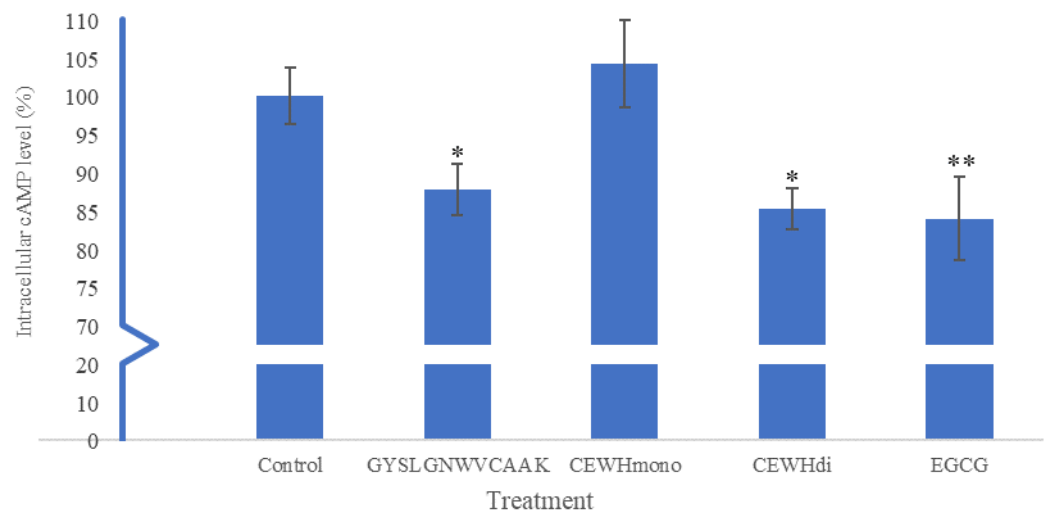


Figure 5. Effects of 10 µg/mL of GYSLGNWVCAAK, CEWH_{mono}, CEWH_{di} and EGCG on the intracellular cAMP level of B16F10 melanoma cells. Note: Results were reported as the mean \pm standard deviation ($n = 3$); * indicates $p < 0.05$ and ** indicates $p < 0.01$, which were significantly different to the untreated control group according to Dunnett's test.

2.6. RT-qPCR Analysis

The effect of cellular treatment with 10 µg/mL of GYSLGNWVCAAK, CEWH_{mono}, CEWH_{di} and EGCG on the mRNA expression level of the *Mitf*, *Tyr*, *Trp-1* and *Trp-2* genes normalized to the untreated control is shown in Table 1. All sample treatments decreased the mRNA expression level of the genes except GYSLGNWVCAAK. The positive control, EGCG, also downregulated all genes similar to sesamol and pyruvic acid [39,40]. Interestingly, treatment of cells with 10 µg/mL of GYSLGNWVCAAK did not alter the mRNA expression of *Mitf* but downregulated the *Tyr* gene with 0.76-fold and upregulated *Trp-1* and *Trp-2* gene with 1.03 and 1.52-fold, respectively. The inconsistency of the results suggests that GYSLGNWVCAAK regulated the tyrosinase family genes independent of each other as well as *Mitf*, as opposed to most reported anti-melanogenesis peptides. Considering that GYSLGNWVCAAK significantly ($p < 0.05$) reduced intracellular tyrosinase activity and the melanin level (Sections 2.3 and 2.4), the peptide was postulated to suppress melanogenesis at the post-translational level instead of at the transcriptional level. For instance, pleiotrophin-treated melanocytes showed reduced protein expression of MITF

and tyrosinase but did not affect the mRNA level of the *Mitf* gene. Pleiotrophin was later found to activate the mitogen-activated protein kinase (MAPK) signalling pathway to induce MITF protein degradation through ubiquitination [41]. For *Trp-1* and *Trp-2* genes, they could be regulated irrespective of *Mitf* and *Tyr* genes [42,43]. Although it is unclear why the genes were regulated independently, the fact that GYSLGNWVCAAK reduced the intracellular cAMP level of B16F10 cells (Section 2.5) could trigger several antagonistic molecular events, i.e., reduced transcriptional activity due to suppression of MITF through the PKA or PI3K signalling pathways, and increased MITF degradation through the MAPK signalling pathway. In short, further investigation is necessary to figure out the anti-melanogenesis mode of action of GYSLGNWVCAAK.

Table 1. Fold change expression of *Mitf*, *Tyr*, *Trp-1* and *Trp-2* genes after treatment with 10 µg/mL of GYSLGNWVCAAK, CEWH_{mono}, CEWH_{di} and EGCG in B16F10 melanoma cells.

Sample	Fold Changes			
	<i>Mitf</i>	<i>Tyr</i>	<i>Trp-1</i>	<i>Trp-2</i>
Control	1.00 (0.88–1.14)	1.00 (0.88–1.13)	1.00 (0.78–1.27)	1.00 (0.88–1.14)
GYSLGNWVCAAK	1.00 (0.97–1.03)	0.76 (0.73–0.80)	1.03 (0.97–1.11)	1.52 (1.48–1.57)
CEWH _{mono}	0.63 (0.59–0.68)	0.60 (0.59–0.61)	0.42 (0.39–0.46)	0.71 (0.68–0.75)
CEWH _{di}	0.88 (0.82–0.95)	0.93 (0.88–0.99)	0.89 (0.88–0.90)	0.71 (0.65–0.80)
EGCG	0.67 (0.60–0.74)	0.58 (0.48–0.71)	0.70 (0.61–0.82)	0.74 (0.59–0.94)

Note: Results were reported as the mean ($n = 3$). The range of fold change is given in the brackets.

For the hydrolysates, CEWH_{mono} and CEWH_{di} suppressed *Mitf*, *Tyr*, *Trp-1* and *Trp-2* genes. Downregulation of the genes by CEWH_{di} could be cAMP-dependent but not for CEWH_{mono} because the hydrolysate did not significantly ($p > 0.05$) reduce the intracellular cAMP level (Section 2.5). CEWH_{mono} was postulated to act independently of cAMP by directly interacting with the members of the PKA, PI3K and/or MAPK signalling pathways. For instance, the fermented microalgae-derived peptide MGRY promoted the activation of ERK in the MAPK signalling pathway, which induced MITF ubiquitination and degradation [44], whereas sesamol advocated the phosphorylation of Akt and GSK3β in the PI3K/Akt/GSK3β pathway to suppress MITF activity [39]. Besides, CEWH_{mono} could act through the Wnt-related integration site (Wnt)/β-catenin signalling pathway since *Mitf* is a downstream target gene of Wnt [45]. Secreted frizzled-related protein 5 (SFRP5) and cardamonin were among the reported anti-pigmentation agents that downregulated melanogenesis-related genes via this pathway without involving cAMP [46]. Inhibition of *Mitf* suppressed the expression of melanogenesis-related genes and, hence, hindered the production of melanin.

3. Materials and Methods

3.1. Materials

Peptide GYSLGNWVCAAK (95.0% purity) was synthesized and purchased from Genscript Biotech Corp., Singapore, whereas the CEW-derived hydrolysates, CEWH_{mono} and CEWH_{di} were prepared according to Yap and Gan [13]. The B16F10 melanoma cell line (ATC.CRL-6475) was purchased from the American Type Culture Collection (ATCC), United States. All chemicals and reagents used in this study were of analytical grade.

3.2. Cell Culture and Maintenance of Cell Line

To revive the frozen cell line, the cells were quickly thawed in a 37 °C water bath and seeded in a T25 cell culture flask containing 8 mL of prewarmed complete growth

medium (CGM). CGM contained Dulbecco's Modified Eagle Medium (DMEM) fortified with 10% foetal bovine serum (FBS) and 1% Penicillin-Streptomycin (PenStrep). The cells were maintained in a 5% CO₂ incubator (MMM Medcenter Einrichtungen GmbH, München, Germany) at 37 °C. The cells were observed under a microscope to check for successful cell attachment and morphological changes. Sub-culturing or passaging of cells was performed once they were grown to approximately 90% confluency and the sub-cultivation ratio used was 1:9. Briefly, the medium was discarded, and the cells were rinsed using 2 mL phosphate-buffered saline (PBS) to remove traces of serum containing protease inhibitors. Then, 1 mL of trypsin–EDTA solution was loaded into the flask and left undisturbed for a few minutes. Cell detachment was checked using a microscope. In total, 2 mL of CGM was added to inhibit the activity of the trypsin–EDTA. The cell suspension was centrifuged at 1200 rpm for 5 min and the supernatant was discarded. For the sub-culture, a pellet of cells was resuspended with an adequate amount of CGM. In total, 1 mL of cells was seeded into each T75 culture flask containing 15 mL prewarmed CGM and then maintained in a 5% CO₂ incubator. To ensure sufficient cell stock for the subsequent analyses, cells from early passages were cryopreserved and 40 cryovials were kept. For cryopreservation, the harvested cell pellet was resuspended in cold, freshly prepared CGM containing 5% DMSO and loaded into a cryovial. The cryovial was kept at −4 °C for 1 h and then at −80 °C for 24 h after which it was kept in a liquid nitrogen tank for long-term storage.

3.3. Cytotoxicity Assay

The cytotoxicity effect of the samples on B16F10 melanoma cells was evaluated through the MTT assay [47]. Briefly, 10⁵ cells per well were seeded in a 96-well plate and incubated for 24 h for cell attachment. The culture media were removed and the cells were rinsed with 200 µL PBS. Next, 100 µL of GYSLGNWVCAAK, CEWH_{mono} and CEWH_{di} (5, 10, 50, 100, 500 and 1000 µg/mL) dissolved in culture media were fed to the cells and then further maintained for 48 h. The treatment was discarded and the cells were rinsed with 200 µL PBS. Then, 20 µL MTT solution (5 mg/mL) was added followed by incubation for 4 h at 37 °C. After incubation, the MTT solution was gently withdrawn without disturbing the MTT formazan precipitate. To dissolve the precipitate, 100 µL of DMSO was loaded with gentle shaking at 100 rpm for 15 min. The absorbance was measured at 570 nm using an ELISA reader (Infinite M200, Tecan, Männedorf, Switzerland). EGCG was used as the positive control. The cell viability was calculated using the equation:

$$\text{Cell viability (\%)} = \frac{A_{\text{sample}}}{A_{\text{control}}} \times 100 \quad (1)$$

where A_{control} was the absorbance of MTT formazan formed without sample treatment, whereas A_{sample} was the absorbance of MTT formazan formed after sample treatment.

3.4. Determination of Intracellular Tyrosinase Activity

The effect of GYSLGNWVCAAK, CEWH_{mono} and CEWH_{di} on the intracellular tyrosinase activity of B16F10 melanoma cells was assessed using the protocol of Kim et al. [48] with slight modifications. Briefly, 10⁵ cells per well were seeded in a 6-well plate and incubated for 24 h to allow cell attachment. The culture media were discarded, then the cells were rinsed with 200 µL PBS. After that, 2 mL of sample (5, 10, 50 and 100 µg/mL) dissolved in culture media was administered and the cells were further incubated for 48 h. The treatment was removed and the cells were rinsed with 200 µL PBS. The cells were collected by trypsinization and the pellet was rinsed again with PBS. To determine the intracellular tyrosinase activity, the pellet was disrupted using 300 µL 20 mM potassium phosphate buffer (pH 6.8) containing 1% Triton X-100 to release tyrosinase from the melanosomes. The cell lysate was kept at −80 °C for 1 h and thawed at room temperature. Then, the lysate was centrifuged at 12,000 rpm for 30 min at 4 °C to collect the supernatant containing the cellular extracts. In a 96-well plate, 20 µL of L-DOPA (2 mg/mL) was added to 80 µL of supernatant and incubated for 1 h at 37 °C. The absorbance was monitored at 475 nm.

EGCG was used as the positive control. The intracellular tyrosinase activity was calculated using the following equation:

$$\text{Intracellular tyrosinase activity (\%)} = \frac{A_{\text{sample}}}{A_{\text{control}}} \times 100 \quad (2)$$

where A_{control} was the absorbance of dopachrome formed without sample treatment, whereas A_{sample} was the absorbance of dopachrome formed after sample treatment.

3.5. Determination of Intracellular Melanin Level

The cells were treated as previously mentioned (Section 2.4). To determine the intracellular melanin level, the pellet was dissolved in 200 μL of 1 M NaOH containing 10% DMSO and heated at 80 $^{\circ}\text{C}$ for 1 h, as previously described by Zhang et al. [49] The absorbance was then monitored at 405 nm using an ELISA reader. EGCG was used as the positive control. The intracellular melanin level was calculated using the following equation:

$$\text{Intracellular melanin level (\%)} = \frac{A_{\text{sample}}}{A_{\text{control}}} \times 100 \quad (3)$$

where A_{control} was the absorbance of melanin without sample treatment whereas A_{sample} was the absorbance of melanin after sample treatment.

3.6. Determination of Intracellular Cyclic Adenosine 3',5'-Monophosphate (cAMP) Level

The cells were treated as above (Section 2.4) and the pellet was subjected to a freeze-thaw cycle for cell lysis. The cells were then centrifuged at 2000 rpm and 4 $^{\circ}\text{C}$ for 20 min. Supernatant was collected for the detection of the intracellular cAMP level using a cAMP ELISA kit (Bioassay Technology Laboratory, Yangpu, Shanghai, China) as per the guidelines provided by the manufacturer. EGCG was used as the positive control.

3.7. Quantitative Reverse Transcription Polymerase Chain Reaction (RT-qPCR)

In a T25 culture flask, 5×10^5 cells were seeded and treated as described above (Section 2.4). The collected cell pellet was immediately stored in -80°C . Total RNA was extracted using a NucleoSpin[®] RNA Kit (Macherey-Nagel, Düren, Germany) according to the manufacturer's instructions. The quality and quantity of the extracted RNA were checked using a Nanodrop 2000c spectrophotometer (Thermo Scientific, Waltham, MA, USA). Reverse transcription of RNA into cDNA was performed using a OneScript[®] Hot cDNA Synthesis Kit (abm Inc., Richmond, BC, Canada), whereas the RT-qPCR was conducted using BlasTaq[™] 2X qPCR MasterMix (abm Inc.). The primer sequences, forward (F) and reverse (R), for *Mitf*, *Tyr*, *Trp-1* and *Trp-2* genes are listed in Table 2.

Table 2. Primer sequences of genes used in the RT-qPCR.

Gene	Primer Sequence	Accession Number
<i>Mitf</i>	F: 5'-TACAGAAAGTAGAGGGAGGAGGACTAAG-3' R: 5'-CACAGTTGGAGTTAAGAGTGAGCATAGCC-3'	NM_008601.3
<i>Tyr</i>	F: 5'-TTGCCACTTCATGTCATCATAGAATATT-3' R: 5'-TTTATCAAAGGTGTGACTGCTATACAAAT-3'	NM_011661.5
<i>Trp-1</i>	F: 5'-GCTGCAGGAGCCTTCTTTCTC-3' R: 5'-AAGACGCTGCACTGCTGGTCT-3'	NM_031202.3
<i>Trp-2</i>	F: 5'-GGATGACCGTGAGCAATGGCC-3' R: 5'-CGGTTGTGACCAATGGGTGCC-3'	NM_010024.3
<i>Gapdh</i>	F: 5'-GCATCTCCCTCACAATTTCCA-3' R: 5'-GTGCAGCGAACTTTATTGATGG-3'	NM_008084.3

The genes of interest were amplified according to the following thermocycling conditions: one cycle of 95 $^{\circ}\text{C}$ for 3 min (DNA polymerase activation) and 40 cycles each

at 95 °C for 15 s (cDNA denaturation) and 60 °C for 1 min (annealing/extension). The relative fold change in gene expression was calculated according to the Livak method of $2^{-(\Delta\Delta C_t)}$ in which a fold change of =, < and >1.0 indicates equal, downregulation and upregulation of gene expression compared to the untreated control group, respectively [50]. The cycle threshold (C_t) value was first normalized to that of the reference gene, *Gapdh* to obtain ΔC_t and then normalized to the C_t of the untreated control to obtain $\Delta\Delta C_t$ using the following equations:

$$\Delta C_{t(\text{sample})} = C_{t(\text{sample})} - C_{t(\text{Gapdh})} \quad (4)$$

$$\Delta C_{t(\text{control})} = C_{t(\text{control})} - C_{t(\text{Gapdh})} \quad (5)$$

$$\Delta\Delta C_t = \Delta C_{t(\text{sample})} - \Delta C_{t(\text{control})} \quad (6)$$

$$\text{Fold change} = 2^{-(\Delta\Delta C_t)} \quad (7)$$

where $C_{t(\text{sample})}$ represents the C_t value after sample treatment; $C_{t(\text{control})}$ represents the C_t value without sample treatment; and $C_{t(\text{Gapdh})}$ represents the C_t value of the reference gene. The result was expressed as a range, which incorporated the standard deviation (sd) of $\Delta\Delta C_t$ into the fold change calculation as follows:

$$\text{Range of fold change} = 2^{-(\Delta\Delta C_t \pm \text{sd})} \quad (8)$$

3.8. Statistical Analysis

Statistical analyses were conducted using IBM SPSS Statistics version 20.0 (SPSS Institute, Chicago, IL, USA). The results were analysed using one-way ANOVA followed by Duncan's post hoc test (Sections 2.3–2.5). Pearson's correlation test was also performed to evaluate the strength of the correlation between intracellular tyrosinase activity and melanin level (Sections 2.4 and 2.5). Dunnett's post hoc test was conducted to compare the means from the experimental groups against the untreated control group (Section 2.6). A p -value of <0.05 implied a significant difference between the sample's means. Each experimental run was performed in triplicate and the result was reported as the mean \pm standard deviation.

4. Conclusions

To summarize the results, GYSLGNWVCAAK, CEWH_{mono} and CEWH_{di} could reduce the intracellular tyrosinase activity and melanin level through the regulation of cAMP level or via the expression of melanogenesis-related genes. Outcomes from the current study could serve as the starting point to understand the underlying complex, multifaceted melanogenesis regulatory mechanism at the cellular level. A comparison of the results using a normal human skin melanocyte model is necessary to justify the anti-pigmentation effect considering that the samples may exhibit opposing effects on human melanocytes [51]. Nonetheless, the cell permeability test and melanosome uptake assay should be conducted to verify the permeability of peptides and hydrolysates. Western blotting analysis could be conducted to demonstrate the translation of melanogenesis regulatory proteins. The regulatory effects of the samples on protein translation, protein degradation, impairment of melanosome maturation or even cell autophagy [52–54] should also be investigated before moving onto animal model or clinical studies.

Author Contributions: Conceptualization, C.-Y.G. and T.-W.W.; methodology, P.-G.Y. and I.N.; software, P.-G.Y. and I.N.; validation, C.-Y.G. and T.-W.W.; formal analysis, I.N.; investigation, P.-G.Y.; resources, C.-Y.G.; data curation, P.-G.Y. and I.N.; writing—original draft preparation, P.-G.Y.; writing—review and editing, C.-Y.G. and T.-W.W.; visualization, P.-G.Y.; supervision, C.-Y.G. and T.-W.W.; project administration, T.-W.W.; funding acquisition, C.-Y.G. All authors have read and agreed to the published version of the manuscript.

Funding: This research was financially supported by Universiti Sains Malaysia RUI Grant (Grant number: 1001/CABR/8011045).

Institutional Review Board Statement: Not applicable.

Informed Consent Statement: Not applicable.

Data Availability Statement: The data related to this research is included in the results section.

Acknowledgments: P.G.Y. would like to thank Raymond Leong for the invaluable advice and support throughout the project.

Conflicts of Interest: The authors declare no conflict of interest.

Sample Availability: Samples of the compounds are not available from the authors.

References

1. Markiewicz, E.; Karaman-Jurukovska, N.; Mammone, T.; Idowu, O.C. Post-inflammatory hyperpigmentation in dark skin: Molecular mechanism and skincare implications. *Clin. Cosmet. Investig. Dermatol.* **2022**, *15*, 2555–2565. [CrossRef] [PubMed]
2. Davis, E.C.; Callender, V.D. Postinflammatory hyperpigmentation: A review of the epidemiology, clinical features, and treatment options in skin of color. *J. Clin. Aesthet. Dermatol.* **2010**, *3*, 20–31. [PubMed]
3. Maghfour, J.; Olayinka, J.; Hamzavi, I.H.; Mohammad, T.F. A Focused review on the pathophysiology of post-inflammatory hyperpigmentation. *Pigment Cell Melanoma Res.* **2022**, *35*, 320–327. [CrossRef] [PubMed]
4. Pillaiyar, T.; Namasivayam, V.; Manickam, M.; Jung, S.H. Inhibitors of melanogenesis: An updated review. *J. Med. Chem.* **2018**, *61*, 7395–7418. [CrossRef]
5. D’Alba, L.; Shawkey, M.D. Melanosomes: Biogenesis, properties, and evolution of an ancient organelle. *Physiol. Rev.* **2019**, *99*, 1–19. [CrossRef]
6. Zolghadri, S.; Bahrami, A.; Hassan Khan, M.T.; Munoz-Munoz, J.; Garcia-Molina, F.; Garcia-Canovas, F.; Saboury, A.A. A comprehensive review on tyrosinase inhibitors. *J. Enzyme Inhib. Med. Chem.* **2019**, *34*, 279–309. [CrossRef]
7. Grand View Research. Skin Lightening Products Market Size, Share & Trends Analysis Report By Product (Cream, Cleanser, Mask), by Nature, by Region, and Segment Forecasts, 2022–2030. Available online: <https://www.grandviewresearch.com/industry-analysis/skin-lightening-products-market> (accessed on 21 November 2022).
8. Agorku, E.S.; Kwaansa-Ansah, E.E.; Voegborlo, R.B.; Amegbletor, P.; Opoku, F. Mercury and hydroquinone content of skin toning creams and cosmetic soaps, and the potential risks to the health of Ghanaian women. *SpringerPlus* **2016**, *5*, 319. [CrossRef]
9. Gbetoh, M.H.; Amyot, M. Mercury, hydroquinone and clobetasol propionate in skin lightening products in West Africa and Canada. *Environ. Res.* **2016**, *150*, 403–410. [CrossRef]
10. Korhonen, H.; Pihlanto, A. Bioactive peptides: Production and functionality. *Int. Dairy J.* **2006**, *16*, 945–960. [CrossRef]
11. Hariri, R.; Saeedi, M.; Akbarzadeh, T. Naturally occurring and synthetic peptides: Efficient tyrosinase inhibitors. *J. Pept. Sci.* **2021**, *27*, e3329. [CrossRef]
12. Song, Y.; Chen, S.; Li, L.; Zeng, Y.; Hu, X. The hypopigmentation mechanism of tyrosinase inhibitory peptides derived from food proteins: An overview. *Molecules* **2022**, *27*, 2710. [CrossRef]
13. Yap, P.G.; Gan, C.Y. Chicken egg white—Advancing from food to skin health therapy: Optimization of hydrolysis condition and identification of tyrosinase inhibitor peptides. *Foods* **2020**, *9*, 1312. [CrossRef]
14. Hong, G.P.; Min, S.G.; Jo, Y.J. Anti-oxidative and anti-aging activities of porcine by-product collagen hydrolysates produced by commercial proteases: Effect of hydrolysis and ultrafiltration. *Molecules* **2019**, *24*, 1104. [CrossRef] [PubMed]
15. Upata, M.; Sirovoharn, T.; Makkhun, S.; Yarnpakdee, S.; Regenstein, J.M.; Wangtueai, S. Tyrosinase inhibitory and antioxidant activity of enzymatic protein hydrolysate from jellyfish (*Lobonema smithii*). *Foods* **2022**, *11*, 615. [CrossRef] [PubMed]
16. Yap, P.G.; Gan, C.Y. Multifunctional tyrosinase inhibitor peptides with copper chelating, UV-absorption and antioxidant activities: Kinetic and docking studies. *Foods* **2021**, *10*, 675. [CrossRef] [PubMed]
17. Feng, Y.X.; Wang, Z.C.; Chen, J.X.; Li, H.R.; Wang, Y.B.; Ren, D.F.; Lu, J. Separation, identification, and molecular docking of tyrosinase inhibitory peptides from the hydrolysates of defatted walnut (*Juglans regia* L.) meal. *Food Chem.* **2021**, *353*, 129471. [CrossRef] [PubMed]
18. Nie, H.; Liu, L.; Yang, H.; Guo, H.; Liu, X.; Tan, Y.; Wang, W.; Quan, J.; Zhu, L. A novel heptapeptide with tyrosinase inhibitory activity identified from a phage display library. *Appl. Biochem. Biotechnol.* **2017**, *181*, 219–232. [CrossRef]
19. Seruggia, D.; Josa, S.; Fernández, A.; Montoliu, L. The structure and function of the mouse tyrosinase locus. *Pigment Cell Melanoma Res.* **2021**, *34*, 212–221. [CrossRef]
20. Bhatnagar, V.; Srirangam, A.; Abburi, R. In vitro modulation of proliferation and melanization of melanoma cells by citrate. *Mol. Cell. Biochem.* **1998**, *187*, 57–65. [CrossRef]
21. Prezioso, J.A.; Wang, N.; Duty, L.; Bloomer, W.D.; Gorelik, E. Enhancement of pulmonary metastasis formation and γ -glutamyltranspeptidase activity in B16 melanoma induced by differentiation in vitro. *Clin. Exp. Metastasis* **1993**, *11*, 263–274. [CrossRef]
22. de Barros, D.P.; Reed, P.; Alves, M.; Santos, R.; Oliva, A. Biocompatibility and antimicrobial activity of nanostructured lipid carriers for topical applications are affected by type of oils used in their composition. *Pharmaceutics* **2021**, *13*, 1950. [CrossRef] [PubMed]
23. Kong, S.; Choi, H.R.; Kim, Y.J.; Lee, Y.S.; Park, K.C.; Kwak, S.Y. Milk protein-derived antioxidant tetrapeptides as potential hypopigmenting agents. *Antioxidants* **2020**, *9*, 1106. [CrossRef] [PubMed]

24. Ochiai, A.; Tanaka, S.; Tanaka, T.; Taniguchi, M. Rice bran protein as a potent source of antimelanogenic peptides with tyrosinase inhibitory activity. *J. Nat. Prod.* **2016**, *79*, 2545–2551. [[CrossRef](#)] [[PubMed](#)]
25. Weisburg, J.H.; Weissman, D.B.; Sedaghat, T.; Babich, H. In vitro cytotoxicity of epigallocatechin gallate and tea extracts to cancerous and normal cells from the human oral cavity. *Basic Clin. Pharmacol. Toxicol.* **2004**, *95*, 191–200. [[CrossRef](#)]
26. Ramsden, C.A.; Riley, P.A. Tyrosinase: The four oxidation states of the active site and their relevance to enzymatic activation, oxidation and inactivation. *Bioorg. Med. Chem.* **2014**, *22*, 2388–2395. [[CrossRef](#)]
27. García-Molina, P.; Muñoz-Munoz, J.L.; Ortuño, J.A.; Rodríguez-López, J.N.; García-Ruiz, P.A.; García-Cánovas, F.; García-Molina, F. Considerations about the continuous assay methods, spectrophotometric and spectrofluorometric, of the monophenolase activity of tyrosinase. *Biomolecules* **2021**, *11*, 1269. [[CrossRef](#)]
28. Hou, H.; Zhao, X.; Li, B.; Zhang, Z.; Zhuang, Y. Inhibition of melanogenic activity by gelatin and polypeptides from pacific cod skin in B16 melanoma cells. *J. Food Biochem.* **2011**, *35*, 1099–1116. [[CrossRef](#)]
29. Chen, Y.P.; Wu, H.T.; Wang, G.H.; Liang, C.H. Improvement of skin condition on skin moisture and anti-melanogenesis by collagen peptides from milkfish (*Chanos chanos*) scales. *IOP Conf. Ser. Mater. Sci. Eng.* **2018**, *382*, 022067. [[CrossRef](#)]
30. Joompang, A.; Jangpromma, N.; Choowongkamon, K.; Payoungkiattikun, W.; Tankrathok, A.; Viyoch, J.; Luangpraditkun, K.; Klaynongsruang, S. Evaluation of tyrosinase inhibitory activity and mechanism of Leucrocine I and its modified peptides. *J. Biosci. Bioeng.* **2020**, *130*, 239–246. [[CrossRef](#)]
31. Wagh, S.; Ramaiah, A.; Subramanian, R.; Govindarajan, R. Melanosomal proteins promote melanin polymerization. *Pigment Cell Res.* **2000**, *13*, 442–448. [[CrossRef](#)]
32. Ancans, J.; Tobin, D.J.; Hoogduijn, M.J.; Smit, N.P.; Wakamatsu, K.; Thody, A.J. Melanosomal pH controls rate of melanogenesis, eumelanin/phaeomelanin ratio and melanosome maturation in melanocytes and melanoma cells. *Exp. Cell Res.* **2001**, *268*, 26–35. [[CrossRef](#)] [[PubMed](#)]
33. Mani, I.; Sharma, V.; Tamboli, I.; Raman, G. Interaction of melanin with proteins— the importance of an acidic intramelanosomal pH. *Pigment Cell Res.* **2001**, *14*, 170–179. [[CrossRef](#)] [[PubMed](#)]
34. Wang, J.; Wang, Y.; Tang, Q.; Wang, Y.; Chang, Y.; Zhao, Q.; Xue, C. Antioxidation activities of low-molecular-weight gelatin hydrolysate isolated from the sea cucumber *Stichopus japonicus*. *J. Ocean Univ. China* **2010**, *9*, 94–98. [[CrossRef](#)]
35. Pongkai, P.; Saisavoey, T.; Sangtanoo, P.; Sangvanich, P.; Karnchanatat, A. Effects of protein hydrolysate from chicken feather meal on tyrosinase activity and melanin formation in B16F10 murine melanoma cells. *Food Sci. Biotechnol.* **2017**, *26*, 1199–1208. [[CrossRef](#)] [[PubMed](#)]
36. Liu, Y.Y.; Su, X.R.; Liu, S.S.; Yang, S.S.; Jiang, C.Y.; Zhang, Y.; Zhang, S. Zebrafish phosvitin-derived peptide Pt5 inhibits melanogenesis via cAMP pathway. *Fish Physiol. Biochem.* **2017**, *43*, 517–525. [[CrossRef](#)]
37. Hu, Z.; Sha, X.; Zhang, L.; Huang, S.; Tu, Z. Effect of grass carp scale collagen peptide FTGML on cAMP-PI3K/Akt and MAPK signaling pathways in B16F10 melanoma cells and correlation between anti-melanin and antioxidant properties. *Foods* **2022**, *11*, 391. [[CrossRef](#)] [[PubMed](#)]
38. Han, J.H.; Bang, J.S.; Choi, Y.J.; Choung, S.Y. Anti-melanogenic effects of oyster hydrolysate in UVB-irradiated C57BL/6J mice and B16F10 melanoma cells via downregulation of cAMP signaling pathway. *J. Ethnopharmacol.* **2019**, *229*, 137–144. [[CrossRef](#)]
39. Wu, P.Y.; You, Y.J.; Liu, Y.J.; Hou, C.W.; Wu, C.S.; Wen, K.C.; Lin, C.Y.; Chiang, H.M. Sesamol inhibited melanogenesis by regulating melanin-related signal transduction in B16F10 cells. *Int. J. Mol. Sci.* **2018**, *19*, 1108. [[CrossRef](#)]
40. Zhou, S.; Sakamoto, K. Pyruvic acid/ethyl pyruvate inhibits melanogenesis in B16F10 melanoma cells through PI3K/AKT, GSK3 β , and ROS-ERK signaling pathways. *Genes Cells* **2019**, *24*, 60–69. [[CrossRef](#)]
41. Choi, W.J.; Kim, M.; Park, J.Y.; Park, T.J.; Kang, H.Y. Pleiotrophin inhibits melanogenesis via Erk1/2-MITF signaling in normal human melanocytes. *Pigment Cell Melanoma Res.* **2015**, *28*, 51–60. [[CrossRef](#)]
42. Zhou, S.; Riadh, D.; Sakamoto, K. Grape extract promoted α -MSH-induced melanogenesis in B16F10 melanoma cells, which was inverse to resveratrol. *Molecules* **2021**, *26*, 5959. [[CrossRef](#)]
43. Kim, J.H.; Sim, G.S.; Bae, J.T.; Oh, J.Y.; Lee, G.S.; Lee, D.H.; Lee, B.C.; Pyo, H.B. Synthesis and anti-melanogenic effects of lipoic acid-polyethylene glycol ester. *J. Pharm. Pharmacol.* **2008**, *60*, 863–870. [[CrossRef](#)] [[PubMed](#)]
44. Oh, G.W.; Ko, S.C.; Heo, S.Y.; Nguyen, V.T.; Kim, G.; Jang, C.H.; Park, W.S.; Choi, I.W.; Qian, Z.J.; Jung, W.K. A novel peptide purified from the fermented microalga *Pavlova lutheri* attenuates oxidative stress and melanogenesis in B16F10 melanoma cells. *Process Biochem.* **2015**, *50*, 1318–1326. [[CrossRef](#)]
45. Steingrímsson, E.; Copeland, N.G.; Jenkins, N.A. Melanocytes and the microphthalmia transcription factor network. *Annu. Rev. Genet.* **2004**, *38*, 365–411. [[CrossRef](#)] [[PubMed](#)]
46. Zou, D.P.; Chen, Y.M.; Zhang, L.Z.; Yuan, X.H.; Zhang, Y.J.; Inggawati, A.; Nguyet, P.T.K.; Gao, W.W.; Chen, J. SFRP5 inhibits melanin synthesis of melanocytes in vitiligo by suppressing the Wnt/ β -catenin signaling. *Genes Dis.* **2021**, *8*, 677–688. [[CrossRef](#)] [[PubMed](#)]
47. Mosmann, T. Rapid colorimetric assay for cellular growth and survival: Application to proliferation and cytotoxicity assays. *J. Immunol. Methods* **1983**, *65*, 55–63. [[CrossRef](#)]
48. Kim, C.S.; Noh, S.G.; Park, Y.; Kang, D.; Chun, P.; Chung, H.Y.; Jung, H.J.; Moon, H.R. A potent tyrosinase inhibitor, (E)-3-(2,4-dihydroxyphenyl)-1-(thiophen-2-yl) prop-2-en-1-one, with anti-melanogenesis properties in α -MSH and IBMX-induced B16F10 melanoma cells. *Molecules* **2018**, *23*, 2725. [[CrossRef](#)]

49. Zhang, X.; Li, J.; Li, Y.; Liu, Z.; Lin, Y.; Huang, J.A. Anti-melanogenic effects of epigallocatechin-3-gallate (EGCG), epicatechin-3-gallate (ECG) and gallic acid (GA) via down-regulation of cAMP/CREB/MITF signaling pathway in B16F10 melanoma cells. *Fitoterapia* **2020**, *145*, 104634. [[CrossRef](#)]
50. Livak, K.J.; Schmittgen, T.D. Analysis of relative gene expression data using real-time quantitative PCR and the $2^{-\Delta\Delta CT}$ method. *Methods* **2001**, *25*, 402–408. [[CrossRef](#)]
51. Zhou, S.; Sakamoto, K. Citric acid promoted melanin synthesis in B16F10 mouse melanoma cells, but inhibited it in human epidermal melanocytes and HMV-II melanoma cells via the GSK3 β / β -catenin signaling pathway. *PLoS ONE* **2020**, *15*, e0243565. [[CrossRef](#)]
52. Campagne, C.; Ripoll, L.; Gilles-Marsens, F.; Raposo, G.; Delevoye, C. AP-1/KIF13A blocking peptides impair melanosome maturation and melanin synthesis. *Int. J. Mol. Sci.* **2018**, *19*, 568. [[CrossRef](#)] [[PubMed](#)]
53. Kim, J.Y.; Kim, J.; Ahn, Y.; Lee, E.J.; Hwang, S.; Almurayshid, A.; Park, K.; Chung, H.W.; Kim, H.J.; Lee, M.S.; et al. Autophagy induction can regulate skin pigmentation by causing melanosome degradation in keratinocytes and melanocytes. *Pigment Cell Melanoma Res.* **2020**, *33*, 403–415. [[CrossRef](#)] [[PubMed](#)]
54. Boo, Y.C. Up-or downregulation of melanin synthesis using amino acids, peptides, and their analogs. *Biomedicines* **2020**, *8*, 322. [[CrossRef](#)] [[PubMed](#)]

Disclaimer/Publisher’s Note: The statements, opinions and data contained in all publications are solely those of the individual author(s) and contributor(s) and not of MDPI and/or the editor(s). MDPI and/or the editor(s) disclaim responsibility for any injury to people or property resulting from any ideas, methods, instructions or products referred to in the content.